

Thermal Insulation Coating Using Natural Stone Powder-Epoxy Composite for Room Temperature Reduction

Redi Bintarto

Ph.D. Student
Mechanical Engineering
Of Brawijaya University
Indonesia

Anindito Purnowidodo

Professor
Mechanical Engineering
Of Brawijaya University
Indonesia

Teguh Dwi Widodo

Assistant Professor
Mechanical Engineering
Of Brawijaya University
Indonesia

Marco Talice

Professor
PM2 Engineering
Italia

Djarot B. Darmadi

Professor
Mechanical Engineering
Of Brawijaya University
Indonesia

The ability of a roof to absorb heat is crucial for maintaining temperature stability within a room. Therefore, natural material composite coatings utilization offers a viable option for modern roof development. This research investigates how using natural stone mixed with epoxy, and applied as a coating on a galvalume surface, influences thermal conductivity and reduces room temperature. Temperature measurements were collected around a small room with a composite-coated roof, utilizing different types of rock in the composition. Thermocouples were placed 20 cm above the roof's surface, attached to the roofing composite, positioned beneath the galvalume layer, and within the small room. The results demonstrate a reduction in thermal conductivity and room temperature when natural stone powder is added to the roof. Experiments using composite coatings with various stone types exhibit varying degrees of room temperature reduction. Consequently, this research concludes that the unique properties of natural stone can effectively lower the thermal conductivity of roofs and decrease room temperature.

Keywords: thermal insulation coating, natural stone, composite, roof technology, temperature reducer, roof coating, galvalume

1. INTRODUCTION

Buildings consume approximately 40% of global energy and are responsible for over 30% of CO₂ emissions [1-4]. A significant portion of this energy goes to maintaining thermal comfort within enclosed spaces, and cooling accounts for around 15% of electricity consumption in buildings [5]. Consequently, temperature regulation is paramount when constructing houses, with the type of roof used playing a substantial role in influencing air temperature, accounting for about 70% of the overall impact. Innovative practices and technologies such as passive cooling techniques employ reflective and radiation processes to achieve comfortable building conditions using natural means to dissipate heat and maintain a pleasant indoor environment [6]. Furthermore, the building materials' thickness impacts the insulation process and energy consumption levels, thus affecting optimization [7,8].

In Indonesia, metal roofs are widely used despite numerous drawbacks, including elevated room temperatures beneath them due to the metal's high thermal conductivity [9]. Research conducted in Ecuador has demonstrated that metal roofs lead to excessive heat buildup in the space below [10].

The increasing number of residents has led to rising demand for cooling, with air conditioners being a popular choice for temperature control [11-14].

However, the widespread use of air conditioners contributes to higher electricity consumption, which is still generated by burning fossil fuels. The overall effect is exacerbating global warming and leading to human discomfort and health issues [15]. Addressing these challenges demands technological solutions, particularly in the form of roof coatings. Implementing coatings that effectively reduce roof temperatures, especially during summer, can be an effective strategy [16,17]. Cool-roofing technology, characterized by high solar reflectance, has proven to be efficient in reducing cooling loads and improving the energy balance of buildings throughout the cooling season [15,18-22]. Composites, particularly those incorporating ceramics, can significantly lower thermal conductivity [23-28].

Using natural materials in composites requires the usage of an adhesive such as epoxy. Epoxy exhibits versatile characteristics and is suitable for surface coatings and adhesives when combined with other materials to create composites for many applications. Epoxy, when used as a resin, along with natural fiber materials, can be employed in composites catering to thermal, mechanical, and electrical requirements [29-31]. Additionally, epoxy's inclusion in the composite can enhance its mechanical properties [32]. Another natural material frequently used for its heat-insulating properties is natural stone. Natural stone finds extensive use in buildings, contributing to aesthetic appeal and thermal comfort [33,34].

Furthermore, natural stones possess the ability to store heat [35]. Metal roof (galvalume) usage in a building's roofing system impacts the necessity for cooling systems and enhances comfort levels by reducing the room temperature. Various methods, like

Received: June 2023, Accepted: July 2023

Correspondence to: Redi Bintarto
Department of Mechanical Engineering,
Brawijaya University, Indonesia
E-mail: redibintarto@ub.ac.id

doi: 10.5937/fme2304457B

© Faculty of Mechanical Engineering, Belgrade. All rights reserved

FME Transactions (2023) 51, 457-469 457

roof coatings application, can minimize heat transfer through the roof [36].

Composite materials, particularly those incorporating ceramics, can significantly lower thermal conductivity [37,38]. Using natural materials in composites requires the usage of an adhesive (epoxy) to bond the raw materials to the galvalume sheet. Epoxy, when used as a resin, along with natural fiber materials, can be employed in composites catering to thermal, mechanical, and electrical requirements [29,39]. Additionally, epoxy's inclusion in the composite can enhance its mechanical properties [32].

Another natural material frequently used for its heat-insulating properties is natural stone. Natural stone finds extensive use in buildings, contributing to aesthetic appeal and thermal comfort [33,40,41]. Furthermore, natural stones possess the ability to store heat [35]. Metal roof (galvalume) usage in a building's roofing system impacts the necessity for cooling systems and enhances comfort levels by reducing the room temperature. Various methods, like roof coatings application, can minimize heat transfer through the roof [36,42].

Based on extensive literature research and the observed impact of galvalume roofs on increasing indoor temperatures and the underutilization of natural stone, there is a clear need for innovation in coating galvalume roofs with natural stone powder composites. This premise raises questions about the composite addition's influence on the galvalume roof's thermal conductivity and its ability to reduce the temperature of the underneath room. Previous research has revealed many published papers on coating roofs of buildings with paint, using non-metallic materials, or studying the ability of pure silicon powder to retain heat. While in this research, we try to utilize the existing natural stone available abundantly in Indonesia.

2. THE COMPOSITE ROOF DESIGNS

2.1 Mechanism of heat transfer of the composite roof system

Heat transfer occurs within a composite roof through the constituent materials, with various transfer mechanisms on the top of the building, such as conduction and radiation. Figure 1 provides a more detailed illustration of these processes.

Heat transfer within a composite roof occurs at both the top and bottom. The top surface experiences radiant heat transfer and convection heat transfer. The formula representing this is written as:

$$Q_s = Q_{rad.out} + Q_{conv.out} + Q_{cond}. \quad (1)$$

Q_s represents the radiative heat from the sun, $Q_{rad.out}$ represents the radiation reflected from the top of the roof layer, and $Q_{conv.out}$ is the convection heat transfer from the top of the roof (in watts, W). Additionally, Q_{cond} refers to the conduction heat transfer that occurs downwards through the roof. On the other hand, the heat transmitted to the underside of the roof occurs primarily through conduction heat transfer, which strongly relies on the thermal conductivity of the roofing material. Therefore, one can compute the heat transferred into the room as follows:

$$Q_{cond} = Q_{rad.in} + Q_{conv.in} + Q_{ve}. \quad (2)$$

Q_{cond} represents the conduction heat transfer within the composite layer of the roof and galvalume (in watts, W). $Q_{rad.in}$ refers to the radiant heat transfer into the room (in W), $Q_{conv.in}$ represents the convection heat transfer into the room (in W), and Q_{ve} is the heat transfer that occurs through the air vent (in W) [36].

By referring to equations 1 and 2, it is evident that Q_{cond} is a type of heat transfer that significantly impacts the temperature within the room under the roof. The idea is to reduce heat transfer by utilizing a roofing material with low thermal conductivity for the top layer.

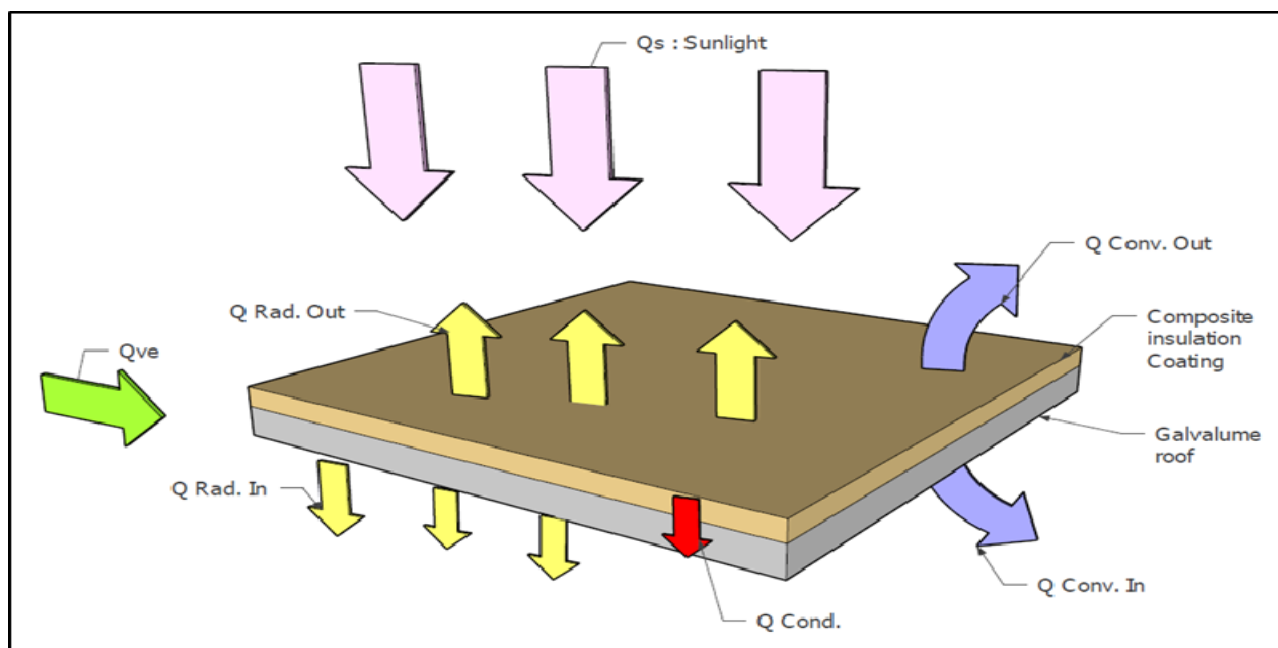


Figure 1. Mechanism of heat transfer of composite roof

Hence, to appropriately address the heat-related issues on the roof and ceiling, it is advisable to apply a coating that can effectively reduce the roof's thermal conductivity [36].

2.2 Composite Thermal Insulation Coating (CTIC)

Composites are versatile materials offering several advantages, including their thermal insulating properties. Their low thermal conductivity [43] and structural strength make them ideal materials for effective thermal insulation. They are particularly suitable for thermal insulation coatings (TIC) on building roofs, and their use can significantly reduce heat transmission into the space below. Heat transfer reduction, in turn, also decreases the use of cooling energy, making layered roofs with heat-reducing properties highly effective in enhancing energy efficiency and comfort within buildings [44]. Therefore, it is crucial to consider the thermal conductivity properties of roofing materials, as the material composition determines the thermal characteristics. Moreover, variations in materials can result in different coating colors, influencing the levels of sunlight absorption and reflection [45,46]. Consequently, all heat transfer mechanisms, including conduction, convection, and radiation, are influenced by the properties of the roofing material.

3. MATERIALS AND METHODS

3.1 Experimental Models

The experiment was conducted over sixteen days, specifically in May and June 2022, between 11:00 a.m. and 1:00 p.m., under hot weather conditions in Malang City (Latitude: -7° 58' 46.92" S & Longitude: 112° 37' 49.44" E), East Java province, Indonesia.

The process started by sorting the natural stone material by size using a rotary shaker. The largest stones remained at the top, while the smaller ones fell to the bottom, following a cascading effect. Subsequently, portions of the so-obtained natural stone powder have been tested to determine their composition and identify the constituent materials present in the rock. Additionally, testing was conducted on the galvalume sheet used, assessing the base level of constituent materials' thermal conductivity. Composition analysis was performed via X-Ray Fluorescence (XRF) testing, and the resulting data allowed us to identify the five larger material components that would impact the thermal conductivity level of the materials.

Subsequently, we created some specimens for running thermal conductivity tests with a coating composition based on predetermined parameters. The chosen specimens' dimensions are per the requirements of the testing equipment, which was a device equipped with 12 thermocouples measuring the heat rate propagation. After applying the composite coating onto the galvalume roofing sheet, several photos were taken to assess the even deposition of the composite material's layer on the roof and to address any color discrepancies resulting from the different types of natural stone material's application.

Six identical miniature rooms (box in the following) were constructed as part of the experiment. Box A served as the reference box, consisting of a box with a galvalume roof without any coating. Box B was coated with epoxy. Boxes C-F were composite-coated galvalume-roof-boxes. The composite material was made of a mixture of natural stone powder and epoxy for the first test (C) and different powder dimensions for the second test (D).

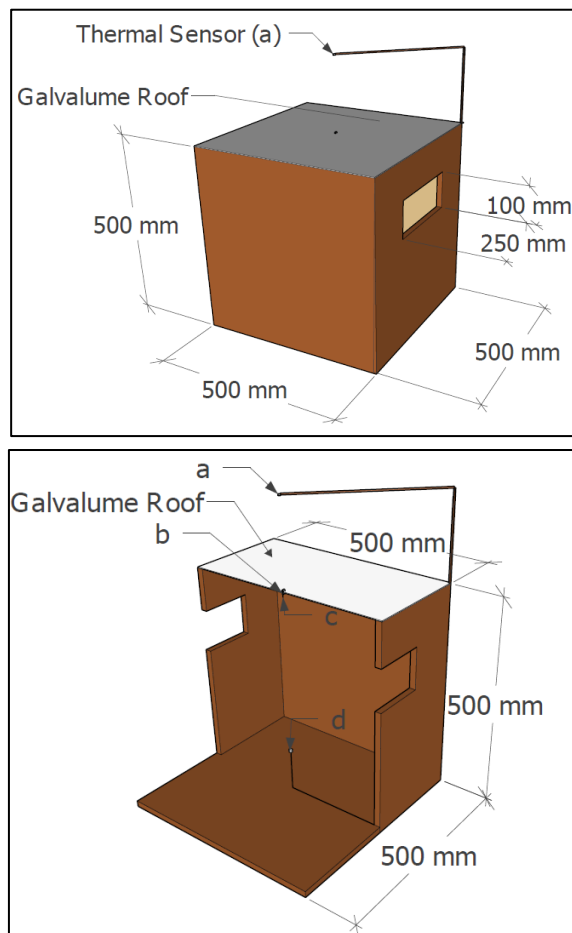


Figure 2. Experiment box

Each box was wood-made, had dimensions of 500 x 500 mm², and was provided with thermocouples at the following measurement points (a) 200mm above the roof, (b) on top of the roof or composite, (c) beneath the galvalume sheet, and (d) at a height of 100mm from the floor, for measuring the room's temperature.

The research focused on utilizing the four natural stones, namely, calcite, dolomite, andesite, and temple. The powder dimensions ranged from 0.05mm to 0.630 mm. The composition of epoxy and natural stones used was 50%:50%.



Figure 3. Experiment tools (temperature data mining)

The specimens (composite roofs) are fabricated using the hand layup method. Epoxy A is mixed with a hardener in a 2:1 ratio (100 grams epoxy:50 grams hardener) - manufactured by PT Justus Kimiaraya.

Table 1. Epoch on epoxy resin specification

Properties	Value	Unit
Viscosity (at 25°C)	13.000±2000	mPa.s
Epoxy number	22.7±0.6	%
Epoxy equivalent	189±5	g/equiv.
Epoxy value	0.53±0.01	equiv./100g
Total chlorine content	<0.2	%
Hydrolyzable chlorine content	<0.05	%
Color according to the Gardner scale	<1	
Density at 25°C	1.17±0.01	g/cm ³
Refractive index at 25°C	1.572±0.003	
Volatile content at 3 h, 140°C	<0.2	%
Vapor Pressure at 80°C	<0.1	mbar
Flashpoint, according to DIN 51584	>250	°C

Table 2. Hardener of epoch on epoxy resin characteristics

Properties	Value	Unit
Viscosity (at 25°C)	0.5-1.0	poise
Active Hydrogen Equivalent Weight	22.7±0.6	g/equiv.
Amine Value	189±5	mg KOH/g
Color according to the Gardner scale	0.53±0.01	Gardner
Density at 25°C	1.17±0.01	g/cm ³

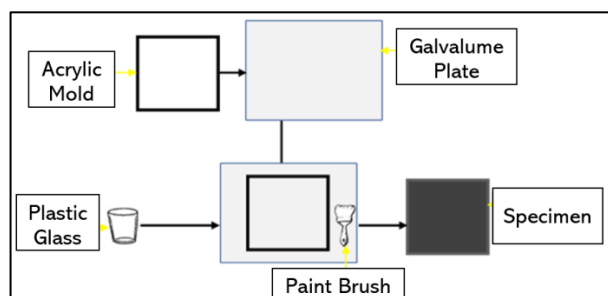


Figure 4. Schematic view of the roof manufacturing process.

Natural stone grains are added to the resin mixture in a 1:1 ratio (150 grams stone:150 grams resin). The mixture is stirred in a mixer at 942 rpm for 300 seconds. Subsequently, it is poured onto the mold-prepared galvalume sheet and brushed evenly to cover the entire surface. The coating is then left to dry. The thickness of the composite roof is in the range of 0.7-0.8 mm.

3.2 Measurement Devices

To ensure the accuracy of the collected data, the thermal conductivity values are measured using a thermal conductivity testing instrument provided by Tokyo Meter Co. Ltd.

Table 3. Thermal Conductivity Measuring Apparatus Specifications

Specifications	
Manufacturer	Tokyo Meter Co. LTD.
Model	VS-40-200SF
Specimen Material	All Solid Materials
Specimen Dimension	40mm Dia. X 4mm
Standard disc (S)	40 mm Dia. (Copper or Copper Alloy)
Temperature Gradient Set Device	
Immersion electric heater	1500W
Max Temperature Thermometer (Digital Indicator)	200°C
Insulator	0-199.9°C
Thermo detector	Glass wool
Thermo detector accurate	C.A thermocouple
Low Temp source	0.1°C
Automatic temperature controller	Chill water bath
	ON-OFF Controller, Magnetic power relay

The apparatus consists of twelve thermocouples, with six sensors positioned on the top of the specimen and the remaining six on its bottom. Additionally, to verify the temperature values recorded by the thermocouples above the roof, tests are conducted at different time intervals using a thermal imager.



Figure 5. Thermal conductivity measuring apparatus.

The coated galvalume specimens were tested using wooden equipment measuring 500 x 500 x 500 mm. The equipment incorporated ventilation according to the guidelines outlined in Regulation of the Minister of Health of the Republic of Indonesia Number 1077 of 2011, which specified a ventilation requirement of 20% of the floor area. Two vents measuring 100 x 250 mm ensured the required ventilation, as illustrated in Figure 2. Figure 3 shows the tools utilized in this study. The specimens were positioned on the test equipment, and thermocouples were installed to measure the environment temperature and the temperature of roof coating, galvalume roof, and room indoor.

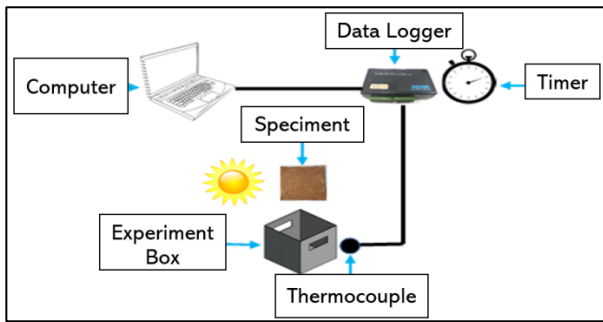


Figure 6. Schematic view of experimental

To ensure the correctness of the temperature readings provided by the thermocouples set above the roof, we conducted additional tests at various times using a thermal imager. Moreover, measurements of solar radiation and wind speed through a solar power meter and an anemometer ensured heat conditions consistency during the tests. These measurements allowed us to collect temperature data on the composite-coated and the non-coated roofs. Figure 7 illustrates the process of data acquisition.

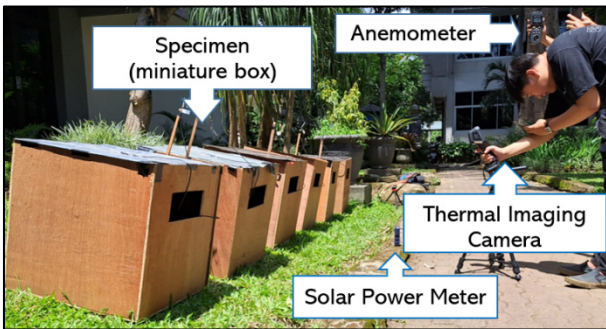


Figure 7. Taking thermal imaging photos

3.3 Evaluation of thermal performance

Multiple indicators are employed to evaluate the impact and advantages of composite coating on galvalume roofs. Roof types B, C, D, E, and F are compared with the reference roof, A, which consists of an uncoated galvalume sheet. The indicators considered are: (i) Effect of composition on the material: Analysing the influence of the composite coating's composition on the material properties. (ii) Roof color after composite coating: Assessing the color variation of the roof surface following the application of the composite coating. (iii) Thermal conductivity: Measuring the ability of the composite-coated and the uncoated galvalume roof to conduct heat. (iv) Roof heat difference using thermal imaging: Utilizing thermal imaging techniques to detect variations in heat distribution between the composite-coated roofs and the uncoated galvalume roof. (v) Room temperature difference: Comparing the temperature variations between the rooms with the composite-coated roofs and the reference room with the uncoated galvalume roof.

Data collection was conducted using DS18B20 temperature sensors integrated with the Arduino system.

Each miniature box was equipped with four sensors placed at different locations to measure the temperature above, directly above, and below the roof, as well as the temperature in the room at 400mm from the roof. The data from all six miniature boxes were simultaneously

tested to ensure real-time observation of any temperature differences.

Table 4. DS18B20 Sensor Specifications

Properties	Value
Model	DS18B20
Specimen Material	189±5
Operating Temperature Range	-55°C to 25°C (-67°F to 257°F)
Temperature accuracy	0.5°C
Power supply range	3.0V-5.5V

4. RESULT AND DISCUSSION

As previously mentioned, this research was conducted during the hottest time of the day in the tropical region. To ensure reliable and predictable results, each data collection process included a miniature box with a roof that lacked a composite layer, serving as a reference. This approach mitigates the potential impact of fluctuations in solar radiation, as any increase or decrease would affect both the experimental and reference miniature boxes, enabling real-time data comparison. Additionally, we have tested various materials to examine the impact of their composition on sunlight absorption and reflection. Consequently, the results of the coatings producing specific colors were also analyzed, as they influence the levels of absorption and reflection.

Heat transfer involves various physical mechanisms, such as radiation from sunlight and convection, the latter associated with mass transfer. Additionally, conduction is another heat transfer mechanism that occurs through solid materials. To assess the impact of conduction heat transfer, a thermal conductivity test is conducted to determine its magnitude.

4.1 Material composition analysis

In general, each type of natural stone possesses a distinct composition of constituent materials, which impacts its thermal conductivity [47-48]; as a result, different natural stone powders for thermal insulation will yield varying results in terms of room temperature.

Table 2 shows the elemental composition of the four natural stones used in the study, ranging from calcite, dolomite andesite, marble, and temple stones. The design of materials could be used as the basis of thermal conductivity value.

When viewed from the composition test carried out, the onyx stone contains a relatively high element of calcium (Ca), which is 96.93%, while marble includes an aspect of calcium (Ca) of 94.41%. From these data, it can be concluded that the role of calcium (Ca) is very influential in decreasing room temperature. At the same time, the dominant elements in andesite and temple stones are elements of calcium (Ca), silicon (Si), and iron (Fe). Andesite has elements of 20.5% (Ca), 28.6% (Si), and 34.5% (Fe). At the same time, the temple stone has features of 23.4% (Ca), 36.7% (Si), and 20.4% (Fe). The presence of silica material is capable of being used as a building roof coating. Silica powder also has excellent thermal insulation ability [49-57].

The design of materials can serve as a basis for determining thermal conductivity values, as the increase

or decrease in thermal conductivity properties often corresponds to similar changes in electrical conductivity for most materials. Applying a silicon coating to the galvalume roof can effectively reduce roof temperature due to the unique characteristics of silicon as a semi-conductor material silicon is widely used for thermal insulation purposes [58], as natural materials with semi-conducting properties can reduce the heat flow rate. When heating occurs within the composite layer, the raw materials will react accordingly. Semiconductor materials like silicon (Si) change their thermal energy content as they exhibit localized temperature behavior, leading to a reduced temperature distribution [59]. Adding silicon to the material composition results in a smaller thermal conductivity[60-61]. So that heat from the sun is not propagated into the room under the roof. The results of the composition test can be seen in Figure 5.

4.2 Macroscopic picture analysis of different natural stones type

In addition to influencing the level of thermal conductivity, the composition of the material also impacts the color of the composite being created. The color, in turn, affects the ability to reflect sunlight. Various types of solar radiation, including UV, visible (Vis), and near-infrared (NIR) radiation, can be reflected. White is the most effective color for reflecting NIR radiation, and this reflection helps to maintain a cooler temperature in the room when exposed to the sun's heat. On the other hand, the visible region of light will be absorbed by the white pigment [62]. Visual analysis of macroscopic photos of natural stone coating specimens was performed to observe the variations in the coatings of each natural stone.

Figure 8 above depicts a photograph of a coating specimen featuring various types of natural stone on a galvalume roof. The six specimen images reveal distinct colors and characteristics for each stone. In images a, b, and c, bright colors are evident, indicating a significant amount of sunlight reflection on the roof. On the other hand, image d, which depicts a mixture of dolomite and epoxy, displays a brown color, suggesting less light reflection compared to images a, b, and c. The remaining two roof types, coated with andesite powder and temple stone with epoxy, appear black, indicating a minimal amount of reflected sunlight. Consequently, the temperature levels experienced by the six roof types differ based on their coating colors. Additionally, the color difference affects the emissivity value of the object's surface, impacting the surface radiation level. This value plays a role in determining the external and internal heat flux of the coated material [63]. It is important to note that bright colors significantly influence the microclimate above the roof, as they reflect more light upward [48].

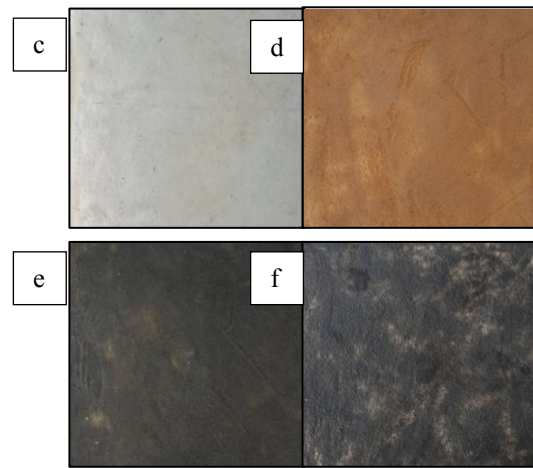
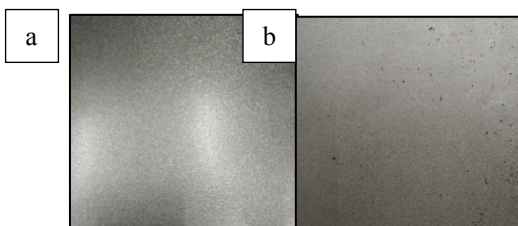


Figure 8. Macroscopic pictures of (a) GR; (b) GRCE; (c) GRCC; (d) GRCD; (e) GRCA; (f) GRCT

This research also captured data using a thermal imager at minutes 4 and 16. The collected data is as follows:

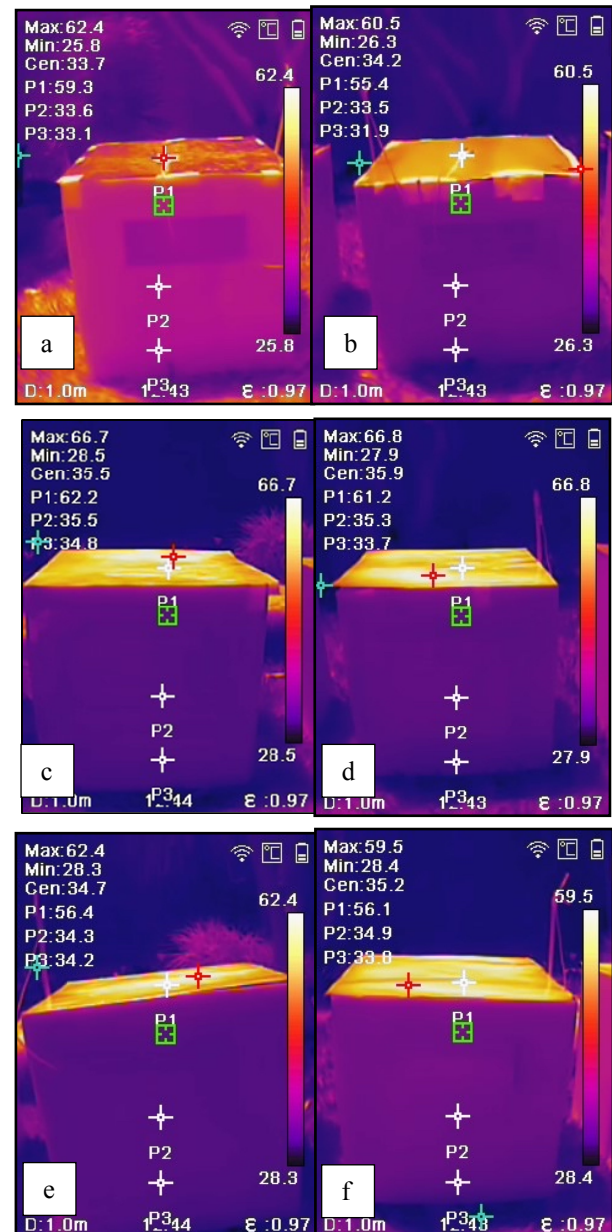


Figure 9. Roof thermal level after 4 minutes; (a) GR; (b) GRCE; (c) GRCC; (d) GRCD; (e) GRCA; (f) GRCT

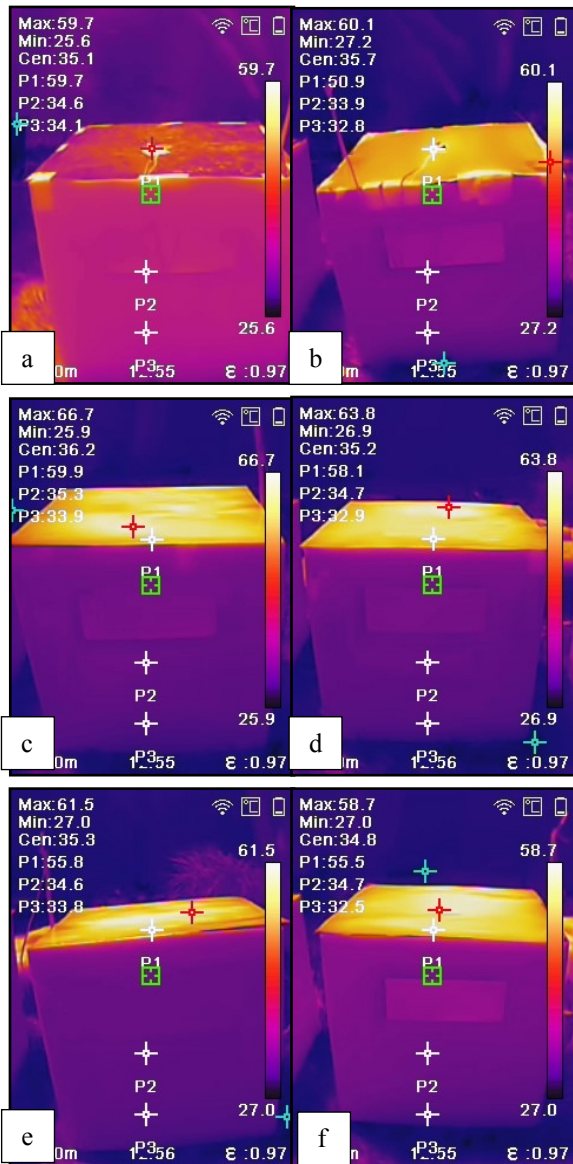


Figure 10. Roof thermal level after 16 minutes; (a) GR; (b) GRCE; (c) GRCC; (d) GRCD; (e) GRCA; (f) GRCT

The thermal imager works by converting infrared into an electrical signal where every object can emit infrared radiation. The hotter an object, the more infrared radiation, so the thermal imager is able to recognize the temperature of an object by capturing the amount of infrared emitted by the object.

Infrared thermography is to convert invisible heat energy into visual, thermal images so that the heat energy emitted from the surface of objects can be seen [64]. But the drawback of the thermal imager is that it is only able to detect the surface of solid and liquid objects, but not gaseous substances, so from the point obtained, only the roof can be used as a benchmark for temperatures that the thermal imager can detect. From the incoming data, it is found that the lowest temperature on the roof is obtained on a roof with only epoxy coating, which is very reasonable because the epoxy is clear like glass so that the heat that hits it will be reflected as much as possible so that the absorption level is small [65].

Coatings using the reflection method are divided into two types, namely solar heat (near infrared) reflecting coating and thermal infrared reflecting coating.

A solar heat-reflecting coating reduces heating by reflecting solar radiation and preventing solar energy from being absorbed on the material's surface. The highest reflection process occurs on objects with white covers coated with transparent pigments. However, this type of coating is unable to absorb infrared radiation effectively. Infrared radiation can only penetrate the first layer and cannot pass through subsequent layers of material [65]. On the other hand, thermal infrared reflecting coatings are specifically designed to minimize thermal emissions and reflect thermal infrared radiation. In this context, aluminum is known for its high reflective strength [65].

Table 5. Thermal Imager Specifications

Tool Specifications	
Manufacturer	HuangzhouMicroimage Software Co., Ltd.
Model	HM-TP52-3AQF/W-B20
Digital Resolution	1600x1200 (2MP)
Image Modes	Thermal/Optical/Fusion/PIP
Measurement Presets	Center spot, Hot spot, Cold spot, User preset point
FOV	37.2o x 50.0o
Thermal sensitivity (NETD)	<40mK,
Spatial resolution (IFOM) accuracy	3.3 mrad +/-2oC
Protection level	IP54

When the galvalume roof is coated solely with epoxy or calcite and dolomite layers, the upper temperature does not differ significantly from the roof's one due to epoxy being a transparent material, which allows sunlight to penetrate the surface of the galvalume metal. Although calcite and dolomite have energy absorption capabilities, their bright white and brown colors result in significant reflections, which lead to a roof's surface temperature being nearly identical to the galvalume metal's value. A notable contrast arises when the composite layer incorporates andesite and temple stone materials.

4.3 Thermal conductivity analysis of different natural stone powder

The thermal conductivity of materials used in building construction is a critical parameter that affects indoor temperature, comfort, and energy conservation [66]. In addition to being influenced by air humidity, the thermal conductivity value of materials directly impacts the indoor temperature. Therefore, selecting materials with appropriate thermal conductivity levels is crucial in determining the energy required for cooling purposes, ultimately affecting electricity consumption[67]. Variations in rock composition will lead to differences in mechanical properties, such as thermal conductivity, and their suitability for thermal insulation purposes. When used for thermal insulation of a building roof, they yield varying outcomes in terms of room temperature [68].

Table 6 presents the thermal conductivity test results for various specimens, including galvalume and natural stone coatings. The thermal conductivity values are as follows: galvalume - 9.39 (W/m²), epoxy-coated

galvalume - 6.66 (W/m²), marble stone coating - 5.60 (W/m²), onyx stone coating - 3.98 (W/m²), andesite stone coating - 2.68 (W/m²), and temple stone coating - 1.46 (W/m²).

Table 6. Roof type and thermal conductivity

roof type	thermal conductivity (W/m ² °C)
A	9.391
B	6.662
C	5.599
D	3.978
E	2.677
F	1.455

This finding demonstrates that galvalume has the highest thermal conductivity value. On the other hand, marble exhibits a higher thermal conductivity value compared to andesite. In contrast, the onyx stone has a lower thermal conductivity value than marble due to its lower iron (Fe) composition. Similarly, the temple stone

possesses a low thermal conductivity value due to its higher silicon (Si) content and lower iron (Fe) content compared to andesite. The findings reveal that the temple stone exhibits the lowest thermal conductivity level, which is predominantly influenced by its composition consisting of 36.7% silicon. Due to their semiconductor properties, natural materials can reduce the heat flow rate. When heating takes place within the composite layer, the raw materials will undergo reactions. Certain materials, such as semiconductors like silicon (Si), can alter the heat energy transfer due to their localized temperature behavior, resulting in a reduced temperature distribution [59]. By adding silicon to the composite, the material's thermal conductivity decreases, preventing the propagation of solar heat into the room beneath the roof [59]. The addition of silicon will reduce the thermal conductivity of the material [29,69] so that heat from the sun is not propagated into the room under the roof, as seen in Figure 5.

Table 7. Description of roof layer used in the experimental work

Roof Type	Materials	Description
A	Galvalume Sheet	3mm galvalume sheet; material compounds: Al 21%; Si 0,3%; P 0,2%; Ca 0,13%; Cr 0,13%; Mn 0,29%; Fe 62,73%; Ni 0,0066%; Zn 14,2%; Br 0,32%; Y 1%; La0,01%; Yb0,06%.
B	Galvalume Sheet, Coated epoxy	Galvalume sheet similar with Type A, coated by mixing Epoxy and hardener type EPH 556. The epoxy mixture is layered 2mm over the galvalume layer evenly and left to dry.
C	Galvalume Sheet, Coated epoxy mixing with calcite powders	Galvalume sheet is like Type A; the coating type contains calcyte stone powders (0.05-0.10mm), and epoxy with ratios of 80% and 20%, whose composite layers thickness is 2mm.
D	Galvalume Sheet, Coated epoxy mixing with dolomite powders	Galvalume sheet is like Type A; the coating type contains dolomite stone powders (0.05-0.10mm), and epoxy with ratios of 80% and 20%, whose composite layers thickness is 2mm.
E	Galvalume Sheet, Coated epoxy mixing with andesite stone powders	Galvalume sheet is like Type A; the coating type contains andhesyte stone powders (0.05-0.10mm), and epoxy with ratios of 80% and 20%, whose composite layers thickness is 2mm.
F	Galvalume Sheet, Coated epoxy mixing with temple stone powders	Galvalume sheet is like Type A; the coating type contains temple stone powders (0.05-0.10mm), and epoxy with ratios of 80% and 20%, whose composite layers thickness is 2mm.

Table 8. Composition of each material

material type	Galvalume	%	Calcite	%	Dolomite	%	Andesite	%	Temple Stone	%
composition	Zn	52.2	Ca	96.93	Ca	94.41	Fe	34.5	Si	36.7
	Fe	22.8	Fe	1.28	Fe	2.51	Si	28.6	Ca	23.4
	Al	17	Sr	0.67	Si	1.2	Al	9.1	Fe	20.4
	Ag	3.1	Yb	0.49	Al	0.88	K	2.34	Al	11
	Y	3	Mo	0.34	Mo	0.49	Ti	2.19	K	4.19

Table 9. Sensor placement and function

Symbol	Sensor Position	Function
a	200mm above roof	measures the air temperature above the roof caused by direct sunlight or reflected sunlight hitting the roof
b	stuck on the roof	measures the temperature of the upper surface of the layer caused by direct sunlight.
c	stuck under the roof	measure the temperature under the roof caused by the conduction process
d	100mm above the floor	measures the temperature that represents the room temperature, where the most suitable position where the occupants are in general is at the bottom of the room

4.4 Thermal level analysis

The thermal analysis consisted in retrieving data over 10 minutes using four temperature sensors. The collected averaged multiple data points were used to generate the plots shown in Fig. 7, enabling a comparison of the recorded temperatures on the computer.

The roof temperature of the calcite powder mixture is slightly lower than that of the epoxy coating. This finding can be due to the higher calcium composition in calcite, which results in lower thermal conductivity and increased heat absorption, thereby reducing light reflection. In the case of the dolomite mixture (roof D), the temperature is lower than that of the calcite mixture due to its yellow-brown color, which reduces brightness and light reflection. Consequently, the heat 20cm above the roof is also lower than in roof C.

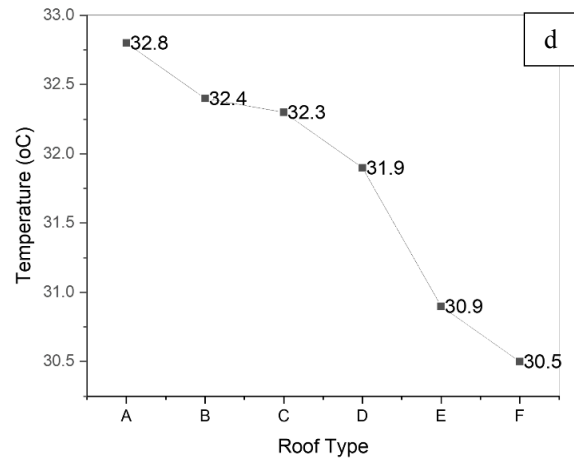
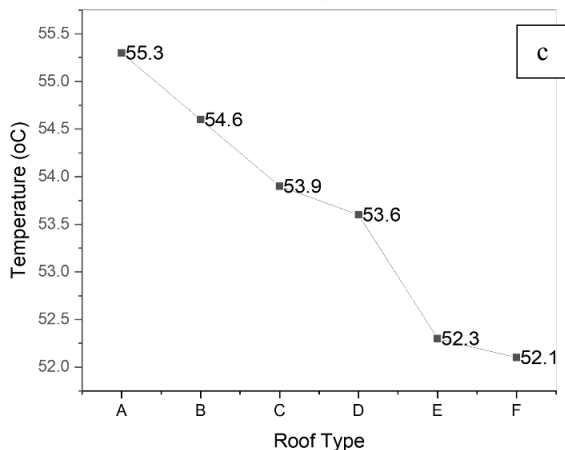
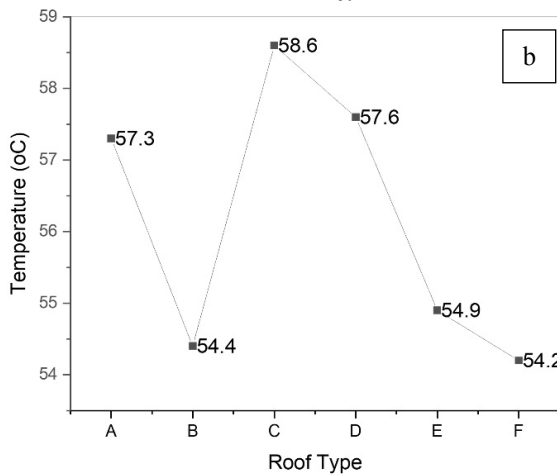
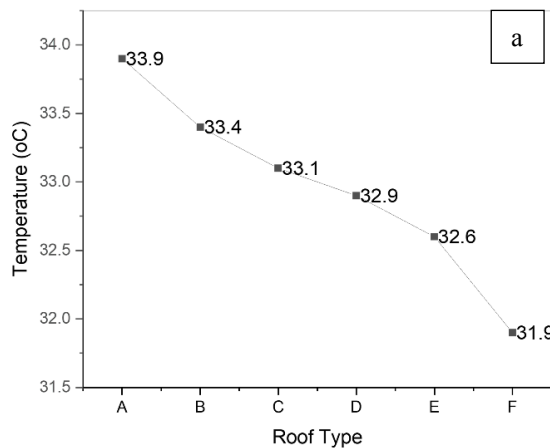


Figure 11. Roof type and average thermal level; (a) Black Square – ATAR; (b) Red Circle - ATSAR (c) Blue up triangle – ATUSR; (d) Green down triangle - ATR

In Figure 5b, the temperature depends upon several factors, such as Q_s , $Q_{rad.out}$, $Q_{conv.out}$, Q_{ve} , and possibly Q_{cond} . The presence of calcium-based materials and added silicon in the composite significantly contributes to heat absorption. In Figure 5c, the temperature recorded by the sensor placed below the roof is typically lower in the presence of a layer of natural stone powder. This finding can depend on the stabilizing effect of natural stone with its diverse compositions, particularly when andesite powder and temple stones are used. In Figure 5d, the addition of a composite layer of natural stone powder results in a lower temperature compared to a galvalume roof without coating. This result indicates that the composite's top layer, consisting of a mixture of natural stones, inhibits heat conduction, as evidenced by smaller thermal conductivity and temperature differences above and below the roof.

5. CONCLUSION

This study provides valuable insights into composite coatings usage on galvalume roofs by leveraging the inherent properties of natural stones to reduce thermal conductivity. The research suggests the following conclusions:

- The composition of natural stones has a direct impact on thermal conductivity. The presence of natural stone powder on the galvalume roof layer influences the heat transfer conduction mechanism on the top surface. Higher semiconductor content, such as Si, in the natural stone composite leads to lower thermal conductivity. Semiconductors exhibit localized temperature behavior and reduce temperature distribution.

- Si content plays a significant role in temperature reduction when applied as a coating on a galvalume roof. Increased Si content results in a more pronounced temperature drop due to reduced heat flow rate. Si's localized temperature behavior helps in minimizing temperature distribution during heating.

- Applying a layer of natural stone composite with low thermal conductivity can effectively reduce heat transfer through conduction on the roof, thereby lowering heat transfer into the room.

For thermal comfort in a room that has a galvalume roof, the addition of natural stone powder impacts the thermal conductivity, offering a reduction of air temperature as a thermal comfort parameter. This research aims to encourage readers and future researchers to investigate further the use of natural stone powder to reduce room temperature and decrease energy consumption for cooling purposes during the summer season.

ACKNOWLEDGMENT

The authors are grateful to Universitas Brawijaya, the Faculty of Engineering, and the Mechanical Engineering Department for funding this research. Special appreciation also goes to the Ministries of Education, Culture, Research, and Technology. The authors would like to acknowledge the valuable contributions of the metal casting laboratory crew throughout this project.

REFERENCES

- [1] L. Yang, H. Yan, and J. C. Lam, "Thermal comfort and building energy consumption implications – A review," *Appl. Energy*, vol. 115, pp. 164–173, 2014.
- [2] D. K. Bhamare, M. K. Rathod, and J. Banerjee, "Passive cooling techniques for building and their applicability in different climatic zones—The state of art," *Energy Build.*, vol. 198, pp. 467–490, 2019.
- [3] V. Chetan, K. Nagaraj, P. S. Kulkarni, S. K. Modi, and U. N. Kempaiah, "Review of Passive Cooling Methods for Buildings," *J. Phys. Conf. Ser.*, vol. 1473, no. 1, 2020.
- [4] R. Bintarto, A. Purnowidodo, D. B. Darmadi, and T. D. Widodo, "The effect of composite thickness as thermal insulation roof coating on room temperature reduction," *Salud, Cienc. y Tecnol.*, vol. 2, no. S2, p. 192, 2023.
- [5] A. Prieto, U. Knaack, T. Auer, and T. Klein, "Passive cooling & climate responsive façade design exploring the limits of passive cooling strategies to improve the performance of commercial buildings in warm climates," *Energy Build.*, vol. 175, pp. 30–47, 2018.
- [6] K. M. Al-obaidi, M. Ismail, A. Malek, and A. Rahman, "Passive cooling techniques through reflective and radiative roofs in tropical houses in Southeast Asia: A literature review," *Front. Archit. Res.*, vol. 3, no. 3, pp. 283–297, 2014.
- [7] N. S. Billington, "Thermal Insulation of Buildings," *Build Serv Eng*, vol. 42, pp. 63–68, 1974.
- [8] B. Givoni, "Indoor temperature reduction by passive cooling systems," *Sol. Energy*, vol. 85, no. 8, pp. 1692–1726, 2011.
- [9] S. Yuliani, G. Hardiman, E. Setyowati, and W. Setyaningsih, "Thermal behaviour of concrete and corrugated zinc green roofs on low-rise housing in the humid tropics," *Archit. Sci. Rev.*, vol. 0, no. 0, pp. 1–15, 2020.
- [10] J. Litardo, J. Macías, R. Hidalgo-León, M. G. Cando, and G. Soriano, "Measuring the effect of local commercial roofing samples on the thermal behavior of a social interest dwelling located in different climates in Ecuador," *ASME Int. Mech. Eng. Congr. Expo. Proc.*, vol. 6, no. November, 2019.
- [11] M. Auffhammer, A. Aroonruengsawat, "Simulating the impacts of climate change, prices and population on California's residential electricity consumption," *Clim. Change*, vol. 109, no. SUPPL. 1, pp. 191–210, 2011.
- [12] J. Huang, K. R. Gurney, "Impact of climate change on U.S. building energy demand: sensitivity to spatiotemporal scales, balance point temperature, and population distribution," *Clim. Change*, vol. 137, no. 1–2, pp. 171–185, 2016.
- [13] S. Sarihi, F. Mehdizadeh Saradj, and M. Faizi, *A Critical Review of Façade Retrofit Measures for Minimizing Heating and Cooling Demand in Existing Buildings*, vol. 64. Elsevier B.V., 2021.
- [14] S. Stevanović, "Optimization of passive solar design strategies: A review," *Renew. Sustain. Energy Rev.*, vol. 25, pp. 177–196, 2013.
- [15] R. Levinson, H. Akbari, S. Konopacki, and S. Bretz, "Inclusion of cool roofs in nonresidential Title 24 prescriptive requirements," *Energy Policy*, vol. 33, no. 2, pp. 151–170, 2005.
- [16] J. Vengala, M. S. Dharek, D. Sachin, T. B. Ghanashyam, "Materials Today: Proceedings The thermal analysis of building model with acrylic and aluminium based roof coating materials," *Mater. Today Proc.*, vol. 47, pp. 3787–3793, 2021.
- [17] I. Oropeza-Perez and P. A. Østergaard, "Active and passive cooling methods for dwellings: A review," *Renew. Sustain. Energy Rev.*, vol. 82, no. July 2016, pp. 531–544, 2018.
- [18] F. Rahmani, M. Alan, M. R. Barzegaran, "International Journal of Electrical Power and Energy Systems Cool roof coating impact on roof-mounted photovoltaic solar modules at texas green power microgrid," *Int. J. Electr. Power Energy Syst.*, vol. 130, no. November 2020, p. 106932, 2021.
- [19] N. Gupta, G. N. Tiwari, "Review of passive heating /cooling systems of buildings," *Energy Sci. Eng.*, vol. 4, no. 5, pp. 305–333, 2016.
- [20] M. Alam, J. Sanjayan, and P. X. W. Zou, *Balancing energy efficiency and heat wave resilience in building design*. Elsevier Inc., 2019.
- [21] R. Levinson, P. Berdahl, H. Akbari, "Solar spectral optical properties of pigments - Part I: Model for deriving scattering and absorption coefficients from transmittance and reflectance measurements," *Sol. Energy Mater. Sol. Cells*, vol. 89, no. 4, pp. 319–349, 2005.
- [22] S. A. Rasheed, A. J. Hasan, "Study of the Immersed Depth on the Natural Convection Heat Transfer from a Heated Triangular Prism Embedded in Porous Media," *FME Trans.*, vol. 50, no. 2, pp. 351–359, 2022.
- [23] J. Adamczyk, R. Dylewski, "The impact of thermal insulation investments on sustainability in the construction sector," *Renew. Sustain. Energy Rev.*, vol. 80, no. September 2016, pp. 421–429, 2017.

- [24] W. Yang, Y. Wang, J. Liu, "Optimization of the thermal conductivity test for building insulation materials under multifactor impact," *Constr. Build. Mater.*, vol. 332, no. 13, p. 127380, 2022.
- [25] F. Amirifard, S. A. Sharif, F. Nasiri, "Application of passive measures for energy conservation in buildings—a review," *Adv. Build. Energy Res.*, vol. 13, no. 2, pp. 282–315, 2019.
- [26] N. Gupta, "Exploring passive cooling potentials in Indian vernacular architecture," *J. Build. Sustain.*, vol. 555, no. 1, pp. 67–69, 2017.
- [27] R. Tang, Y. Etzion, "On thermal performance of an improved roof pond for cooling buildings," *Build. Environ.*, vol. 39, no. 2, pp. 201–209, 2004.
- [28] J. Testa, M. Krarti, "A review of benefits and limitations of static and switchable cool roof systems," *Renew. Sustain. Energy Rev.*, vol. 77, no. October 2016, pp. 451–460, 2017.
- [29] N. Saba, M. Jawaid, O. Y. Alothman, "Recent advances in epoxy resin, natural fiber-reinforced epoxy composites and their applications," 2015.
- [30] M. Dinulović, B. Rašuo, A. Slavković, G. Zajić, "Flutter Analysis of Tapered Composite Fins: Analysis and Experiment," *FME Trans.*, vol. 50, no. 3, pp. 576–585, 2022.
- [31] E. Sulistyono, "V. 03 n. 1," no. 3, pp. 15–23, 2022.
- [32] A. M. López-Buendía, C. Guillem, J. M. Cuevas, F. Mateos, and M. Montoto, "Natural stone reinforcement of discontinuities with resin for industrial processing," *Eng. Geol.*, vol. 166, pp. 39–51, 2013.
- [33] B. Tufan, M. Kun, "Thermal Insulation Performance and Thermal Conductivity Evaluation of Natural Stones by Infrared Thermography," no. 62, pp. 1–9, 2014.
- [34] R. Bintarto, N. Hamidi, R. Raharjo, T. Dwi Widodo, "Effect of Machining Parameters on the Surface Roughness of Dolomite Cups," *IOP Conf. Ser. Mater. Sci. Eng.*, vol. 494, no. 1, 2019.
- [35] R. Tiskatine *et al.*, "Suitability and characteristics of rocks for sensible heat storage in CSP plants," *Sol. Energy Mater. Sol. Cells*, vol. 169, no. May, pp. 245–257, 2017.
- [36] M. C. Yew, N. H. R. Sulong, W. T. Chong, S. C. Poh, B. C. Ang, and K. H. Tan, "Integration of thermal insulation coating and moving-air-cavity in a cool roof system for attic temperature reduction," *Energy Convers. Manag.*, vol. 75, pp. 241–248, 2013.
- [37] K. Muthukumar, R. V. Sabariraj, S. D. Kumar, and T. Sathish, "Materials Today: Proceedings Investigation of thermal conductivity and thermal resistance analysis on different combination of natural fiber composites of Banana, Pineapple and Jute," *Mater. Today Proc.*, vol. 21, pp. 976–980, 2020.
- [38] J. Hu *et al.*, "Polymer composite with enhanced thermal conductivity and mechanical strength through orientation manipulating of BN," *Compos. Sci. Technol.*, vol. 160, pp. 127–137, 2018.
- [39] S. Polymer, M. Composite, and M. Application, "V. 02 n. 1," no. 1, pp. 1–8, 2021.
- [40] D. Medjelekh, L. Ulmet, S. Abdou, and F. Dubois, "A field study of thermal and hygric inertia and its effects on indoor thermal comfort: Characterization of travertine stone envelope," *Build. Environ.*, vol. 106, pp. 57–77, 2016.
- [41] M. S. Hatamipour and A. Abedi, "Passive cooling systems in buildings: Some useful experiences from ancient architecture for natural cooling in a hot and humid region," *Energy Convers. Manag.*, vol. 49, no. 8, pp. 2317–2323, 2008.
- [42] K. Sun, W. Zhang, Z. Zeng, R. Levinson, M. Wei, and T. Hong, "Passive cooling designs to improve heat resilience of homes in underserved and vulnerable communities," *Energy Build.*, vol. 252, p. 111383, 2021.
- [43] A. D. La Rosa *et al.*, "Environmental impacts and thermal insulation performance of innovative composite solutions for building applications," *Constr. Build. Mater.*, vol. 55, pp. 406–414, 2014.
- [44] A. Synnefa, M. Santamouris, H. Akbari, "Estimating the effect of using cool coatings on energy loads and thermal comfort in residential buildings in various climatic conditions," *Energy Build.*, vol. 39, no. 11, pp. 1167–1174, 2007.
- [45] R. Levinson, H. Akbari, P. Berdahl, K. Wood, W. Skilton, and J. Petersheim, "A novel technique for the production of cool colored concrete tile and asphalt shingle roofing products," *Sol. Energy Mater. Sol. Cells*, vol. 94, no. 6, pp. 946–954, 2010.
- [46] G. Habtay, J. Buzas, and I. Farkas, "Heat Transfer analysis in the chimney of the indirect solar dryer under natural convection mode," *FME Trans.*, vol. 48, no. 3, pp. 701–706, 2020.
- [47] Y. A. Popov, D. F. C. Pribnow, J. H. Sass, C. F. Williams, and H. Burkhardt, "Characterization of rock thermal conductivity by high-resolution optical scanning," *Geothermics*, vol. 28, no. 2, pp. 253–276, 1999.
- [48] M. Santamouris, A. Synnefa, T. Karlessi, "Using advanced cool materials in the urban built environment to mitigate heat islands and improve thermal comfort conditions," *Sol. Energy*, vol. 85, no. 12, pp. 3085–3102, 2011.
- [49] H. Abe, I. Abe, K. Sato, M. Naito, "Dry powder processing of fibrous fumed silica compacts for thermal insulation," *J. Am. Ceram. Soc.*, vol. 88, no. 5, pp. 1359–1361, 2005.
- [50] I. Abe, K. Sato, H. Abe, M. Naito, "Formation of porous fumed silica coating on the surface of glass fibers by a dry mechanical processing technique," *Adv. Powder Technol.*, vol. 19, no. 4, pp. 311–320, 2008.
- [51] H. Du *et al.*, "The dual effect of zirconia fiber on the insulation and mechanical performance of the fumed silica-based thermal insulation material," *Ceram. Int.*, vol. 48, no. 5, pp. 6657–6662, 2022.
- [52] H. Yang *et al.*, "Multifunctional wood based composite phase change materials for magnetic-thermal and solar-thermal energy conversion and storage," *Energy Convers. Manag.*, vol. 200, no. June, p. 112029, 2019.

[53] J. Feng *et al.*, "Study of thermal stability of fumed silica based thermal insulating composites at high temperatures," *Compos. Part B Eng.*, vol. 42, no. 7, pp. 1821–1825, 2011.

[54] J. Feng, D. Chen, W. Ni, S. Yang, and Z. Hu, "Study of IR absorption properties of fumed silica-opacifier composites," *J. Non. Cryst. Solids*, vol. 356, no. 9–10, pp. 480–483, 2010.

[55] Y. Lei, X. Chen, H. Song, Z. Hu, and B. Cao, "Improvement of thermal insulation performance of silica aerogels by Al₂O₃ powders doping," *Ceram. Int.*, vol. 43, no. 14, pp. 10799–10804, 2017.

[56] C. Li, Z. Chen, W. Dong, L. Lin, and X. Zhu, "A review of silicon-based aerogel thermal insulation materials: Performance optimization through composition and microstructure," *J. Non. Cryst. Solids*, volume 553, no. November 2020, p. 120517, 2021.

[57] T. W. Lian, A. Kondo, T. Kozawa, T. Ohmura, W. H. Tuan, and M. Naito, "Effect of fumed silica properties on the thermal insulation performance of fibrous compact," *Ceram. Int.*, vol. 41, no. 8, pp. 9966–9971, 2015.

[58] S. Shafi, J. Tian, R. Navik, Y. Gai, X. Ding, and Y. Zhao, "Fume silica improves the insulating and mechanical performance of silica aerogel/glass fiber composite," *J. Supercrit. Fluids*, vol. 148, no. December 2018, pp. 9–15, 2019.

[59] W. Moritz, T. Yoshinobu, F. Finger, S. Krause, M. Martin-fernandez, M. J. Schöning, "High resolution LAPS using amorphous silicon as the semiconductor material," vol. 103, pp. 436–441, 2004.

[60] T. N. Singh, S. Sinha, V. K. Singh, "Prediction of thermal conductivity of rock through physico-mechanical properties," *Build. Environ.*, vol. 42, no. 1, pp. 146–155, 2007.

[61] G. Loke, W. Yan, T. Khudiyev, G. Noel, Y. Fink, "Recent Progress and Perspectives of Thermally Drawn Multimaterial Fiber Electronics," vol. 1904911, pp. 1–30, 2019.

[62] O. Sandin, J. Nordin, M. Jonsson, "Reflective properties of hollow microspheres in cool roof coatings," *J. Coatings Technol. Res.*, vol. 14, no. 4, pp. 817–821, 2017.

[63] Z. Charqui, L. El Moutaouakil, M. Boukendil, R. Hidki, "International Journal of Thermal Sciences Numerical study of heat transfer in a tall, partitioned cavity confining two different fluids: Application to the water Trombe wall," *Int. J. Therm. Sci.*, vol. 171, no. August 2021, p. 107266, 2022.

[64] A. Taheri-Garavand *et al.*, "An intelligent approach for cooling radiator fault diagnosis based on infrared thermal image processing technique," *Appl. Therm. Eng.*, volume 87, pp. 434–443, 2015.

[65] R. F. Brady, V. Wake, "Principles and fo ~ lations for organic coatings with tailored infrared properties," vol. 20, pp. 1–25, 1992.

[66] L. Aditya *et al.*, "A review on insulation materials for energy conservation in buildings," vol. 73, no. August 2015, pp. 1352–1365, 2017.

[67] "2022 Measurement and identification of temperature-dependent thermal".

[68] A. Yamamoto, H. Miyazaki, and T. Takeuchi, "Thermoelectric properties of Al- (Mn , X) -Si C54-phase (X 5 Ru and Re)," vol. 023708, pp. 0–10, 2014.

[69] B. Benane *et al.*, "Multiscale structure of super insulation nano-fumed silicas studied by SAXS, tomography and porosimetry," *Acta Mater.*, vol. 168, pp. 401–410, 2019.

NOMENCLATURE

TIC	Thermal Insulation Coating
GR	Galvalume roof
GRCE	Galvalume roof-coated epoxy
GRCC	GRCE and calcite stone powder
GRCD	GRCE and dolomite stone powder
GRCA	GRCE and andesite stone powder
GRCT	GRCE and temple stone powder.
ATAR	Average Temperature at 200 mm Above the Roof
ATSAR	Average Temperature above (stick on) the roof or composite
ATUSR	Average Temperature under the (stick-on) roof
ART	Average Room Temperature – at 400 mm under the roof

Symbols

Q _s	Sun heat radiation [W]
Grad. out	Radiative heat reflected from the top of the roof [W]
Q _{cov. out}	Convective heat transfer from the top of the roof [W]
Q _{cond.}	Conductive heat transfer of roof [W]
Grad. in	Radiative heat transfer to inside the box [W]
Q _{cov. in}	Convective heat transfer to underneath the box [W]
Q _{ve}	Heat transfer due to ventilation [W]
k	Thermal Conductivity [W/m.K]

ТЕРМОИЗОЛАЦИОНИ ПРЕМАЗ КОРИШЋЕЊЕМ ПРИРОДНОГ КАМЕНА У ПРАХУ И ЕПОКСИДНОГ КОМПОЗИТА ЗА СМАЊЕЊЕ СОБНЕ ТЕМПЕРАТУРЕ

Р. Бинтарто, А. Пуровидодо, Т.Д. Видодо,
М. Талиће, Ђ.Б. Дармади

Способност крова да апсорбује топлоту је кључна за одржавање температурне стабилности у просторији. Стога, коришћење композитних премаза од природних материјала нуди одрживу опцију за савремени развој кровова. Ово истраживање истражује како коришћење природног камена помешаног са епок-

сидом и нанешеног као премаза на површини од галвалума утиче на топлотну проводљивост и смањује собну температуру. Мерења температуре су прикупљена око мале просторије са кровом обложеним композитом, користећи различите врсте стена у композицији. Термопарови су постављени 20 цм изнад површине крова, причвршћени за кровни композит, позиционирани испод слоја галвалума и унутар мале просторије. Резултати показују смањење топ-

лотне проводљивости и собне температуре када се на кров дода прах природног камена. Експерименти са композитним премазима са различитим врстама камена показују различите степене смањења собне температуре. Сходно томе, ово истраживање закључује да јединствена својства природног камена могу ефикасно смањити топлотну проводљивост кровова и смањити собну температуру.